HYDROGEN
JURNAL KEPENDIDIKAN KIMIA
https://e-journal.undikma.ac.id/index.php/hydrogen/index

December 2025. 13(6)
e-ISSN: 2656-3061
p-ISSN: 2338-6487
pp. 1141-1154

Utilization of Rice Husk Waste in PVA-Based Hydrogel Formulation

Gilar Wisnu Hardi*, Sari Artauli Lumban Toruan, Nurohmat, Berlian Kusuma Dewi, Suci Nurjanah, Bachtiar Efendi, Winani
Politeknik Negeri Indramayu, Indramayu, 45252, Indonesia
* Corresponding Author e-mail: gilarwisnu@polindra.ac.id

Article History
Received: 02-12-2025
Revised: 23-12-2025
Published: 31-12-2025

Keywords: Hydrogel; Polyvinyl Alcohol (PVA); Rice Husk Cellulose; Agglomeration; Mechanical Failure.

Abstract
The development of sustainable and cost-effective biomaterials is a primary focus in modern biomedical engineering. Addressing the critical need for circular economy solutions, this study introduces a novel ternary hydrogel composite integrating cellulose extracted from rice husk waste into a Polyvinyl Alcohol (PVA) and Guar Gum (GG) matrix. Cellulose was successfully extracted through alkalization and bleaching processes, with FTIR analysis confirming the removal of lignin and hemicellulose. The optimization of the hydrogel matrix demonstrated that a composition of 12.5% PVA and 1% Guar Gum (F2) exhibited superior mechanical properties, achieving a Tensile Strength (TS) of 10.49 MPa and Elongation at Break (EB) of 271.17%. However, the incorporation of rice husk cellulose (F3) unexpectedly resulted in a significant reduction in mechanical integrity, with TS dropping to 5.48 MPa. Uniquely, this research elucidates the mechanistic origin of this trade-off: SEM analysis provided definitive evidence that the failure was attributed to severe cellulose agglomeration and poor interfacial adhesion, which acted as structural defects. Furthermore, the study reveals a critical artifact where structural failure correlated with an increased Swelling Ratio (245.8%), proving that the observed high-water uptake was driven by passive void filling rather than true network hydrophilicity. The study concludes that while rice husk is a viable source of cellulose, simple solution blending is insufficient for reinforcement. Future research must prioritize high-energy dispersion techniques to overcome agglomeration and realize the material's potential for biomedical applications.

How to Cite: Hardi, G. W., Toruan, S. A. L., Nurohmat, Dewi, B. K., Nurjanah, S., Efendi, B., & Winani. (2025). Utilization of Rice Husk Waste in PVA-Based Hydrogel Formulation. Hydrogen: Jurnal Kependidikan Kimia, 13(6), 1141–1154. https://doi.org/10.33394/hjkk.v13i6.18632

https://doi.org/10.33394/hjkk.v13i6.18632

INTRODUCTION

The development of advanced biomaterials from sustainable and low-cost resources is a primary focus in modern biomedical engineering. Hydrogels, as three-dimensional polymer networks capable of absorbing and retaining large quantities of water, have become materials of choice for various biomedical applications, including wound dressings, drug delivery, and tissue engineering. These unique properties are attributed to their ability to mimic the native extracellular matrix (ECM), high biocompatibility, and tunable porosity (Mohanty et al., 2025).

Among various synthetic polymers, Polyvinyl Alcohol (PVA) has been used extensively for hydrogel formulation. PVA possesses excellent biocompatibility, is non-toxic, and can be easily processed into hydrogels via an environmentally friendly physical crosslinking method: the freeze-thaw (F-T) cycle. This method is highly sought after as it avoids the use of potentially cytotoxic chemical crosslinking agents (such as glutaraldehyde), thus yielding a safer product for biological contact (Tamahkar & Ozkahraman, 2015).

Despite these advantages, pure PVA hydrogels often exhibit significant drawbacks, primarily poor mechanical integrity (low tensile strength and tear resistance). These weak mechanical properties limit their application in areas requiring handling or sustaining physiological loads

(Chen et al., 2017). To overcome this, the most common strategy is to develop composite hydrogels by incorporating fillers or natural polymers to enhance the network's strength. In line with the principles of a circular economy, the utilization of agricultural waste as a source for biopolymer fillers has become highly attractive. Rice husk, an abundant by-product of rice milling, is a rich (containing 35-45%) and very low-cost source of cellulose (Alonso-Cuevas et al., 2025).

Cellulose is known as a robust, hydrophilic, and biocompatible biopolymer. Theoretically, the abundant hydroxyl -OH groups on the cellulose surface can form strong hydrogen bonds with PVA chains, acting as an effective reinforcement agent to improve the hydrogel's mechanical properties (M. Wang et al., 2022). However, the transition from theory to practice presents significant engineering challenges. Unlike pristine bacterial cellulose, cellulose extracted from lignocellulosic biomass often consists of micro-sized particles with broad size distributions and high surface energy. A critical bottleneck in utilizing such fillers is their strong tendency to self-associate and agglomerate within viscous polymer solutions (G. Wang et al., 2022). This phenomenon is problematic because agglomeration reduces the effective interfacial area for stress transfer and creates structural discontinuities (voids) within the hydrogel matrix, which can paradoxically weaken the material instead of reinforcing it. Therefore, addressing the practical issue of filler dispersion is crucial for realizing the potential of agricultural waste in biomedicine.

This study investigates the integration of extracted Rice Husk Cellulose (RHC) into a modified PVA/Guar Gum matrix. Beyond simple formulation, this research aims to explicitly analyze the interplay between processing methods, filler agglomeration, and the resulting physicochemical properties. By elucidating the mechanism behind the trade-off between mechanical strength and swelling capacity, this study seeks to establish the critical processing parameters required to utilize rice husk cellulose effectively, thereby determining its suitability for specific biomedical applications such as absorbent wound dressings.

METHOD

Cellulose Extraction from Rice Husk

Cellulose extraction from rice husk waste was performed via a multi-stage chemical delignification process, modified from previous methods (Irianto et al., 2024). This process consisted of physical preparation, alkali treatment (alkalinization), and bleaching. First, the raw feedstock (rice husk) was washed thoroughly with running water to remove physical contaminants and debris. The material was then dried at ambient temperature (±25°C) for 24 hours, followed by mechanical grinding and sieving to obtain a fine powder (passing a 40-mesh sieve). The first chemical stage was alkalinization, which aims to remove hemicellulose and part of the lignin. The feedstock powder was immersed in a 5% (w/v) sodium hydroxide (NaOH) solution at a 1:25 solid-to-liquid ratio (w/v). NaOH was selected as the primary delignification agent due to its ability to disrupt the lignocellulosic structure; it effectively saponifies the intermolecular ester bonds linking hemicellulose and lignin, rendering them soluble while inducing cellulose swelling to increase accessibility. This suspension was heated to 80°C for 2 hours under continuous stirring (Paramitha & Maharani, 2025).

After the reaction, the resulting black liquor was discarded, and the remaining pulp was rinsed repeatedly with deionized water until a neutral pH was achieved. The second stage was bleaching, designed to completely remove residual lignin. The alkali-treated pulp was steeped in a 1.7% (w/v) sodium chlorite ($NaClO_2$) solution. This solution was prepared in an acetate buffer (pH 4.5-5) composed of 0.2 M acetic acid and sodium hydroxide (Farrukh et al., 2025).

Sodium chlorite was chosen over other oxidative agents (such as hydrogen peroxide or elemental chlorine) because of its high selectivity; it targets lignin phenolic groups via oxidative cleavage without causing severe depolymerization of the cellulose chains, thereby preserving the fiber aspect ratio essential for mechanical reinforcement. The bleaching reaction was conducted at 70°C for 2 hours. This bleaching procedure (2-hour heating) was repeated five times to ensure complete delignification, which was indicated by the fibers turning pure white. Finally, the resulting purified cellulose was washed thoroughly with deionized water to remove all residual chemical reagents (solubilized lignin, hemicellulose, and chlorine ions).

The resulting high-purity cellulose microparticles were dried prior to use. Obtaining high-purity cellulose via this method is critical, as the removal of non-cellulosic components enhances the surface exposure of hydroxyl groups, which theoretically facilitates hydrogen bonding with the PVA matrix. However, the physical state of this extracted cellulose during mixing will play a decisive role in dispersion homogeneity, directly influencing the tensile strength and water absorption capacity of the final composite hydrogel.

Synthesis of Composite Hydrogels

Composite hydrogels were synthesized using a solution blending method followed by physical crosslinking via freeze-thaw (F-T) cycles. The specific formulation consisted of 12.5% (w/v) PVA as the primary polymer matrix, 1% (w/v) rice husk cellulose as the filler, and 2% (w/v) PEG-400 and 1% (w/v) Glycerol as plasticizers (Górska et al., 2024). The synthesis procedure commenced by dissolving 13.75 g of PVA in approximately 60–70 mL of deionized water (DI water) within a beaker. The solution was heated to 80°C on a hotplate under magnetic stirring for 60 minutes, or until the PVA was completely dissolved and the solution became clear. Following dissolution, the PVA solution was cooled to ~40 °C. Subsequently, plasticizers were added. 2.20 g (≈1.96 mL) of PEG-400 and 1.10 g (≈0.87 mL) of Glycerol were added sequentially to the cooled PVA solution.

After each addition, the solution was stirred for 10–15 minutes to ensure homogeneity. In the cellulose incorporation stage, 1.10 g of rice husk cellulose powder (previously prepared as a suspension in a small amount of water) was gradually added to the PVA/PEG/Glycerin matrix solution. This addition was performed under vigorous stirring at 40 °C to prevent agglomeration. To ensure thorough particle dispersion, the mixture was stirred for an additional 15–30 minutes and subjected to brief sonication. Finally, the solution's volume was adjusted (q.s.) to a final volume of 110 mL with DI water and stirred once more. The homogeneous hydrogel precursor solution was then cast into mold. To induce physical crosslinking, the molds were subjected to three F-T cycles, consisting of a freezing phase at −20 °C for 16 hours, followed by a thawing phase at ambient temperature (±25 °C) for 8 hours. After the third cycle, the former hydrogels were demolded and dried in an oven at 50 °C for 9 hours, or until a constant dry weight was achieved.

Hydrogel Characterization

Swelling Test

Swelling tests were performed to evaluate the hydrogel's ability to absorb and retain water, a fundamental parameter in determining its swelling ratio (SR) (Ahmed, 2015). The test procedure was conducted using a gravimetric method (Stan et al., 2025). Dried hydrogel samples were first weighed to obtain the initial dry weight (W0). Subsequently, the samples were immersed in 8 mL of deionized water at room temperature.

To observe the water absorption kinetics, the samples were retrieved at time intervals of 5, 15, 25, 35, 45, 55, and 60 minutes. At each point, the sample was removed, excess surface water was gently blotted off (e.g., using filter paper), and it was immediately weighed to obtain the

swollen weight (Wt) (Elsaeed et al., 2022). The percentage Swelling Ratio (SR) was calculated using the following formula:

$$\text{SR (\%)} = \frac{Wt - W0}{W0} x100\%$$

While, W0 is Initial dry weight of the hydrogel and Wt :is weight of the swollen hydrogel at time t.

Mechanical Properties Test

Evaluation of the hydrogels' mechanical properties is essential to quantify their ability to withstand external forces, including compression, tension, and shear. This characterization is particularly crucial for biomedical applications—such as wound dressings, tissue implants, and tissue engineering scaffolds—where the material must possess sufficient mechanical integrity to maintain its structural form and ensure functional performance under physiological loads (Ahearne, 2022).

Tensile Strength Test

Tensile testing was performed to quantify the hydrogels' mechanical properties under uniaxial tension. Samples were precisely cut into a standard dumbbell geometry and securely mounted onto the grips of a Universal Testing Machine (UTM). A tensile force was applied at a constant strain rate until the sample experienced mechanical failure (rupture). Key parameters derived from the resulting stress-strain curve included the ultimate tensile strength (UTS) (MPa), elongation at break (%), and Young's Modulus (MPa) (Lin et al., 2022).

Scanning Electron Microscopy (SEM)

Scanning Electron Microscopy (SEM) was employed to investigate the porous architecture and surface morphology of the hydrogels. The analysis focused on comparing the microstructure of the pristine PVA hydrogel with that of the composite hydrogel containing rice husk cellulose. Key parameters examined included the homogeneity of the rice husk cellulose dispersion within the PVA matrix, the resulting pore size, shape, and distribution, and the presence of any structural defects, such as cracks or voids, within the material (Lee et al., 2024).

FTIR (Fourier Transform Infrared Spectroscopy)

FTIR spectroscopy was employed to identify characteristic functional groups and to elucidate the intermolecular interactions between the PVA and rice husk cellulose components. The analysis focused on detecting potential spectral peak shifts (e.g., in the hydroxyl -OH region) which would signify chemical interactions, such as hydrogen bonding. This method also served to confirm the presence and successful incorporation of the rice husk cellulose within the final composite hydrogel matrix (Himawan et al., 2025).

RESULTS AND DISCUSSION

SEM Analysis of Raw Rice Husk

SEM analysis of the raw rice husk surface (Figure 1) reveals a morphology that is distinctly different from that of rice straw. As observed, the surface is highly structured, uneven, and covered with complex, overlapping protrusions (undulations and papillae). These small, prominent oval or round structures covering the surface are scientifically known as silica bodies or papillae (Hoerudin et al., 2022). Rice husk is well-known for its exceptionally high inorganic silica (SiO_2) content, which can account for up to 20% of its dry weight. This silica is embedded within the epidermis (outermost layer) in a highly organized pattern, serving as a physical and biological shield for the rice grain within (Shivasharanappa et al., 2022).

The overlapping, flake-like layers are the lignocellulosic epidermis itself, while the visible gaps and voids are likely stomata (pores) and crevices between the rigid silica bodies (Hoerudin et al., 2022; Shivasharanappa et al., 2022). The comparison to rice straw is accurate. Rice straw (the stalk) has a more fibrous structure, composed of vascular bundles. In contrast, rice husk (the hull) has a rigid, dense, silica-rich epidermal structure. This is precisely why the rice husk morphology (Figure 1) appears far more complex and "structured" (Sinamo et al., n.d.).

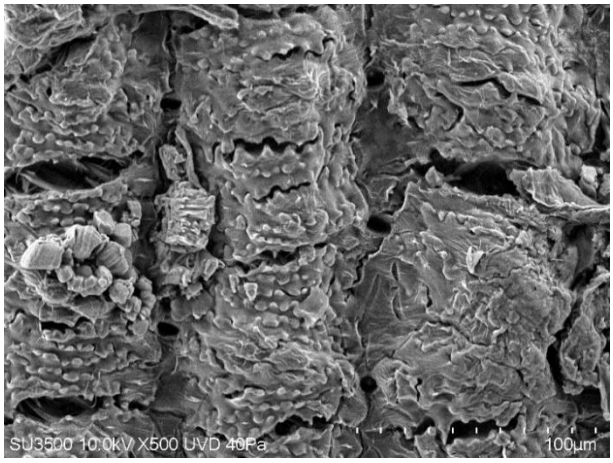

Figure 1**.** SEM morphology of the outer surface of rice husk (500x) showing the silica-rich papillae structure.

This dense, silica-layered structure makes the rice husk highly resistant to chemical penetration (such as NaOH). The alkalinization (delignification) process must not only dissolve lignin and hemicellulose but must also struggle to penetrate this rigid silica barrier. More importantly, the silica (SiO_2) itself is insoluble in the standard extraction process (NaOH and $NaClO_2$). If it is not removed via specialized treatments (e.g., hydrothermal or strong acid leaching), this residual silica will remain and contaminate the final cellulose product (Park et al., 2023). Crucially, if the extraction is incomplete, these impurities will alter the surface chemistry of the resulting cellulose fibers. In the subsequent hydrogel formation, such surface heterogeneity often drives the cellulose to self-associate rather than disperse. This acts as a precursor to the particle agglomeration observed in the composite hydrogels, which—as discussed in later sections—is the primary cause of mechanical failure. The SEM image (Figure 1) confirms this highly organized, silica-rich structure. This implies that the greatest challenge in its utilization lies not with the cellulose itself, but with the removal of its silica contaminant. If this residual silica is carried into the PVA hydrogel, it will act as a defect (like an agglomerate), weakening the mechanical properties and compromising the material's biocompatibility, thereby rendering it unsuitable for medical applications.

FTIR Analysis of Rice Husk Cellulose

FTIR analysis was performed on the Rice Husk (SP) sample to confirm its chemical identity and to verify the success of the extraction (delignification and bleaching) process. The FTIR spectrum of the SP sample (Figure 2) exhibits a distinct profile characteristic of pure cellulose, confirmed via two primary aspects: (1) the presence of characteristic cellulose peaks, and (2) the absence of impurity peaks (lignin and hemicellulose). The most important evidence of a successful extraction is what is absent from the spectrum, as the alkalization (5% NaOH) and bleaching ($NaClO_2$) processes were specifically designed to dissolve and remove hemicellulose and lignin. The spectrum shows no significant peak in the ~1730–1735 cm^{-1} region, which represents the C=O (carbonyl/ester) stretching vibrations from hemicellulose (Adawiyah et al., 2022); the absence of this peak proves the alkali (NaOH) treatment successfully hydrolysed and dissolved it. Furthermore, the spectrum lacks a sharp peak around ~1510–1515 cm^{-1},

characteristic of the aromatic ring (C=C) vibrations in lignin, confirming the bleaching process successfully removed it (Azzouni et al., 2024).

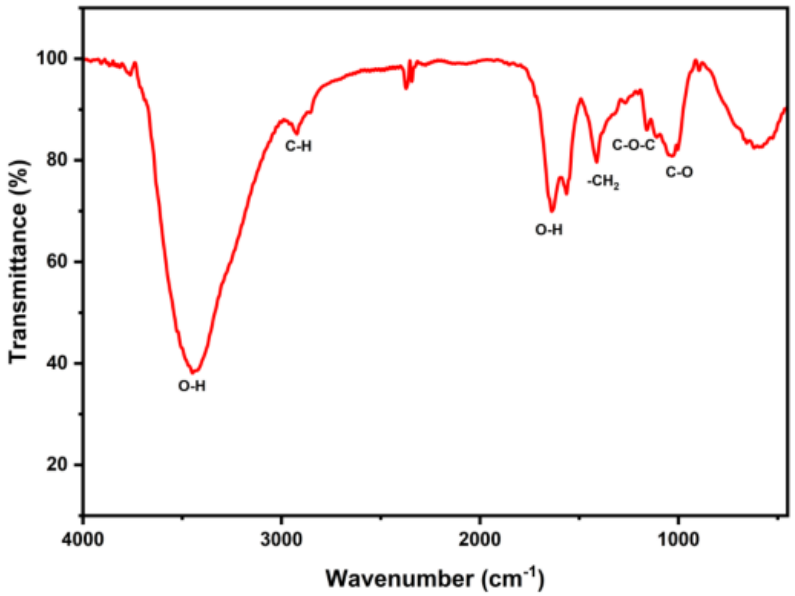

Figure 2. FTIR Spectrum of Rice Husk Cellulose

Successful purification is further supported by the dominance of peaks identical to Type I cellulose (Mamudu et al., 2025). This includes the very broad and strong O-H band (~3448 cm^{-1}), indicating an extensive network of inter- and intramolecular hydrogen bonds crucial for subsequent interaction with the PVA matrix, and the standard aliphatic C-H band (~2922 cm^{-1}). The minor peak at ~1637 cm^{-1} represents the O-H bending vibrations of strongly adsorbed water molecules (Dai et al., 2023). Finally, the polysaccharide "fingerprint" region (1200–1000 cm^{-1}) confirms the structure: the sharp peak at ~1159 cm^{-1} represents the asymmetric C-O-C stretching of the β-glycosidic linkages (the cellulose backbone), and the strong peak at ~1031 cm^{-1} is the C-O stretching of the primary alcohol on the glucose ring. Therefore, this FTIR analysis confirms that the two-stage extraction process successfully converted the raw rice husk (rich in silica, lignin, and hemicellulose) into pure cellulose with a high degree of purity.

Hydrogel Characterization

Swelling Ratio Analysis

The water uptake capacity, or swelling ratio (SR), is a fundamental parameter of hydrogels that dictates their water retention capability and relevance for biomedical applications, such as exudate-absorbing wound dressings (R. Wang et al., 2024). The equilibrium swelling ratio (at 60 minutes) for the rice husk-based formulations is summarized in Table 1.

Table 1. Equilibrium Swelling Ratio (SR%) Results (60 Minutes)

Sample Code (Formulation)	W0 (g)	Ws (g)	Swelling Ratio (SR%)
F1: PVA/PEG/Glycerin/Rice Husk Cellulose	0.35	0.82	134.2%
F2: PVA/Guar Gum/PEG/Glycerin (Matrix)	0.58	1.52	162.1%
F3: F2 + Rice Husk Cellulose	0.24	0.83	245.8%
F4: F2 + Chitosan (Comparator)	0.31	2.21	612.9%

Data analysis revealed a critical and interesting outcome. The PVA/Guar Gum base matrix (F2) exhibited an equilibrium SR of 162.1%. However, when rice husk cellulose was added to the PVA matrix without Guar Gum (F1), the swelling ratio (SR) unexpectedly decreased to

134.2%. This seemingly counter-intuitive result (where adding a hydrophilic filler decreases SR) is a commonly reported phenomenon. Cellulose, especially in microcrystalline form, acts not only as a hydrophilic filler but also as a potent physical crosslinking agent (Q. Wang et al., 2022). The abundant hydroxyl (-OH) groups on the cellulose surface form extensive hydrogen bonds with the PVA chains. In the context of biomedical applications, this phenomenon presents a trade-off. For wound dressings aimed at high-exudate wounds (e.g., severe burns), this reduced swelling capacity is disadvantageous as it limits fluid management. However, for applications requiring dimensional stability or sustained drug delivery, this tighter network structure is beneficial as it prevents rapid disintegration and controls the diffusion rate of bioactive agents (Liu & Chan, n.d.).

The most significant finding was observed in formulation F3. When rice husk cellulose was added to the matrix already containing Guar Gum (F2), the SR sharply increased from 162.1% (F2) to 245.8% (F3). This result indicates a strong synergistic effect between PVA, Guar Gum (GG), and Rice Husk Cellulose. Unlike in F1 (where cellulose likely agglomerated and "constricted" the PVA matrix), in F3, Guar Gum also a polysaccharide likely acted as a stabilizer and dispersing agent (Mieles-Gómez et al., 2021). During the blending process, GG presumably prevented the rice husk cellulose particles from agglomerating. This homogeneous dispersion is critical: instead of acting as dense, rigid crosslinkers (as in F1), the cellulose and GG particles together formed a more organized and potentially more porous 3D architecture. Consequently, the maximum number of hydrophilic (-OH) groups from both cellulose and Guar Gum were exposed to water molecules, drastically improving the hydrogel's water holding capacity (WHC). The increase in swelling in F3 was accompanied by a notable decline in structural integrity (tensile strength). This inverse relationship—high swelling but low strength—indicates that the swelling was not driven by network expansion, but rather by the formation of structural defects.

As a comparator, formulation F4 (which replaced cellulose with chitosan) demonstrated the absolute highest SR (612.9%), classifying it as a superabsorbent polymer (SAP). This massive increase is attributed to Chitosan fundamentally different nature. Cellulose and Guar Gum are neutral polysaccharides. In contrast, chitosan is a cationic polyelectrolyte (T. Zhao et al., 2021). In an aqueous medium (neutral or slightly acidic), the primary amine ($-NH_2$) groups on chitosan become protonated into cationic ammonium ($-NH_3$) groups. These positive changes along the polymer chains create strong electrostatic repulsion, forcing the network to uncoil and expand massively. Furthermore, these ions generate strong osmotic pressure that draws large quantities of water molecules into the matrix (Merisha et al., 2025; T. Zhao et al., 2021). This swelling study demonstrates that the addition of rice husk cellulose alone (F1) is counterproductive. However, the inclusion of Guar Gum (F2) was crucial as a dispersing additive, allowing the cellulose (F3) to be effectively exposed and creating a synergy that enhanced water uptake. For maximum water absorption capacity, chitosan (F4) was the superior additive due to its polyelectrolyte swelling mechanism.

The inclusion of cellulose into the viscous PVA/Guar Gum matrix led to significant filler agglomeration, attributed to the strong tendency of cellulose fibers to self-associate and the insufficiency of magnetic stirring to disperse them within the viscous F3 mixture. Instead of reinforcing the hydrogel, these agglomerates acted as stress concentrators that disrupted the continuity of the polymer network, creating interfacial voids and gaps between the filler and the matrix. This microstructural defect resulted in a dual phenomenon: the voids allowed for the passive entrapment of bulk water, artificially inflating the swelling ratio (anomalous swelling), while the lack of effective stress transfer caused the material to fracture prematurely under tensile load. These results confirm that simple solution blending is inadequate for dispersing lignocellulosic fillers in viscous matrices; therefore, future research must employ high-energy processing techniques, such as ultrasonication or high-shear homogenization, to

break down agglomerates and ensure the homogeneous distribution required for true network reinforcement.

Tensile Test Result

Evaluation of the mechanical properties (Table 3) reveals fundamental findings regarding the inter-component interactions within the dried hydrogel, which is crucial for determining the material's structural integrity (Uchida et al., 2025). The analysis shows a remarkable synergy between PVA and Guar Gum (GG), wherein the addition of 1% GG (Formulation F2) dramatically doubles the tensile strength (TS) to 10.49 MPa and increases elongation (EB) to 271.17%, compared to the F1 control (pure PVA, TS 5.22 MPa). This indicates that GG actively participates in the formation of the physical crosslink network, likely through extensive hydrogen bonding with the PVA chains, resulting in a robust base matrix (S. Wang et al., 2024).

Table 2. Mechanical Test Results

Sample Code (Formulation)	Tensile Strength (TS) (MPa)	Elongation at Break (EB) (%)
PVA/PEG/Glyserin (F1)	5,22 ± 0,27	188,04 ± 42,44
PVA/Guargum/PEG/Glyserin (F2)	10,49 ± 6,24	271,17 ± 107,03
PVA/Guargum/PEG/Glycerin/Celulose Rice Husk (F3)	5,48 ± 0,39	176,87 ± 27,42
PVA/Chitosan/Guargum/PEG/Glycerin (F4)	0,95 ± 0,23	99,27 ± 24,29

However, the most critical finding is the catastrophic detrimental effect of cellulose addition. The initial hypothesis that cellulose would act as a reinforcement was disproven; conversely, the addition of rice husk cellulose (F3) caused mechanical failure, dropping the TS back to 5.48 MPa and EB to 176.87%. This definitively proves that the cellulose failed to integrate and instead acted as a structural defect. This phenomenon is classically attributed to poor filler dispersion (agglomeration), wherein the non-dispersed cellulose clumps create stress concentration points, causing premature crack propagation at points of poor interfacial adhesion and material failure at low stress (Somseemee et al., 2022). The most extreme case was F5 (Chitosan), which exhibited the worst mechanical performance (TS 0.95 MPa), highlighting the extreme trade-off between superabsorbent swelling capacity and fragile structural integrity.

SEM Morphology of Composite Hydrogel

SEM analysis (Figure c) provides crucial visual evidence for understanding the physical properties of the F3 composite (PVA/Guargum/PEG/Glycerin/Rice Husk Cellulose), whose surface exhibits "bubbles" not present in F1 or F2.

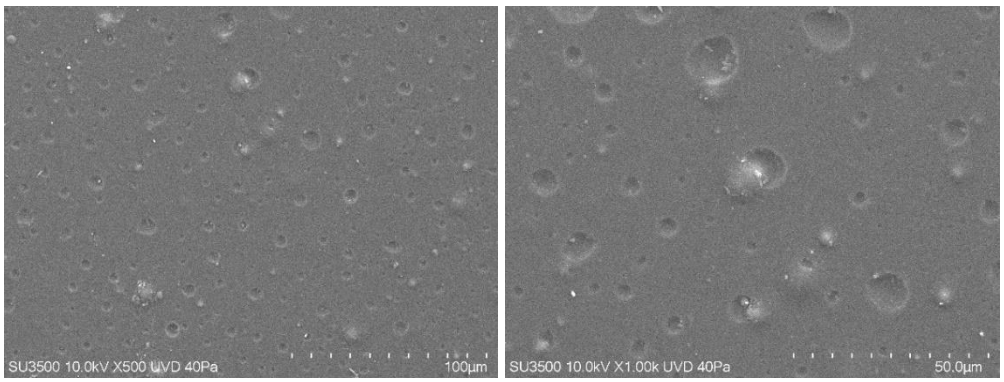

Figure 3. SEM Morphology of Composite Hydrogel

The formation of these bubbles is exclusively attributed to the addition of the rice husk cellulose filler into the high-viscosity polymer matrix (PVA/Guar Gum). This viscosity, combined with simple stirring, failed to "wet" the cellulose particles, leading to significant agglomeration and air entrapment (Sultana et al., 2023). These 5.30 μm voids are not functional pores, but rather severe structural defects.

The consequences are critical and twofold: First, these defects act as stress concentration points, which directly explains the mechanical failure (the drastic TS decrease from 10.49 MPa to 5.48 MPa) as cracks propagate from these weak voids (Sørensen, 2024). Second, these defects also explain the "Swelling Paradox": The high SR (245.8%) in F3 is proven to be an artifact, not caused by polymer absorption, but rather by the passive filling of water via capillary action into these pre-existing voids and internal cracks (Z. Zhao et al., 2025). Thus, this SEM image is the key evidence proving that the failure of cellulose dispersion (agglomeration) simultaneously caused low mechanical strength and an artificially high swelling ratio.

FTIR Analysis of Composite Hydrogels

FTIR analysis of the F3 composite hydrogel (PVA/Guar gum/PEG/Glycerine/Rice Husk Cellulose) (Figure 4) was performed to confirm the molecular interactions between components. As expected, the resulting spectrum is dominated by signals from the majority matrix component, PVA (12.5%), evident from the strong C-O stretching bands at ~1111 & ~1033 cm^{-1} and the C-H stretching at ~2926 cm^{-1}. Characteristic peaks from the minor components (1% Cellulose and 1% Guar Gum), such as the C-O-C β glycosidic stretching of cellulose (~1159 cm^{-1}), are largely “masked” by the much stronger PVA and PEG signals, a common superposition phenomenon in composite spectra (Brand, 2020).

The most Important analytical point is the very broad and strong O-H absorption band at ~3448 cm^{-1}, which is definitive proof of an extensive hydrogen-bonding (H-bond) network. This confirms that all components (PVA, Cellulose, GG, PEG) are chemically compatible and possess the potential to interact (Guo et al., 2010).

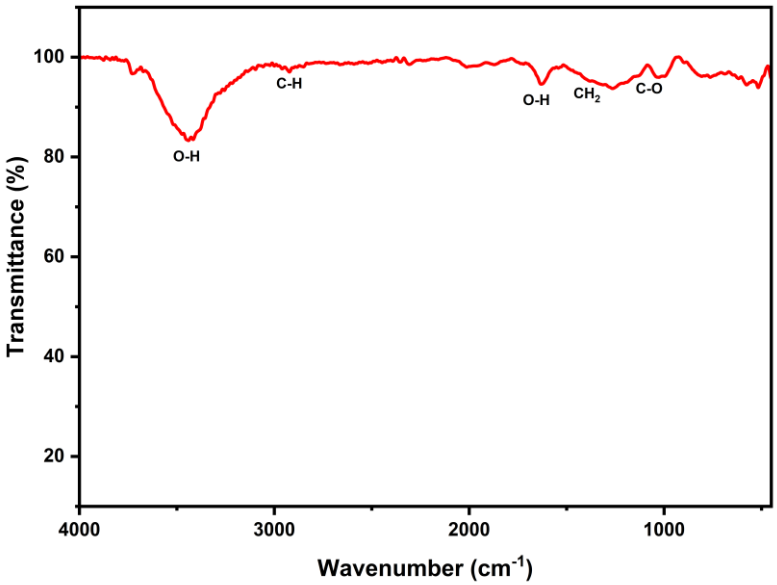

Figure 4. FTIR spectrum results of Sample 3

However, a critical analysis emerges when this 'bulk' FTIR data—which indicates bonding potential—is integrated with the microscopic (SEM) and mechanical (Tensile Test) data. The Tensile Test data (Table 3) proves that this material mechanically failed (TS dropped

drastically to 5.48 MPa), and the SEM data (Figure 1.5.3) proves it failed to disperse physically (severe cellulose agglomeration occurred). Therefore, the combined conclusion is: the strong hydrogen bonds detected by FTIR (~3448 cm^{-1}) likely formed predominantly within two separate phases—strong internal bonds within the PVA/GG matrix, and strong internal bonds within the cellulose agglomerates themselves. The mechanical failure (TS 5.48 MPa) and the interfacial cracks seen in the SEM occurred due to a lack of interfacial H-bonds between these two phases (Hishikawa et al., 2017). Thus, FTIR confirmed the chemical potential, but the failure in physical processing (dispersion) prevented this potential from being realized, leading to poor interfacial adhesion and structural failure.

CONCLUSION

This study successfully extracted pure cellulose from rice husk waste, confirmed by FTIR analysis to be free of lignin and hemicellulose, and optimized a Polyvinyl Alcohol (PVA)/Guar Gum hydrogel matrix (F2) that exhibited superior mechanical synergy (TS 10.49 MPa; EB 271.17%). However, the incorporation of rice husk cellulose (F3) revealed a critical failure in simple solution blending, resulting in a drastic reduction in tensile strength to 5.48 MPa. The novelty of this research lies in the mechanistic elucidation of this failure: unlike conventional studies that often equate high swelling with superior hydrophilicity, this study identified that the increased Swelling Ratio (245.8%) in F3 was a structural artifact. SEM analysis confirmed that this "anomalous swelling" was driven by the passive entrapment of water into micro-voids created by severe cellulose agglomeration, rather than true polymer network expansion.

The significant impact of this study is the demonstration that chemical compatibility (hydrogen bonding potential) is insufficient to guarantee composite performance if hydrodynamic barriers are not addressed. It highlights a critical processing bottleneck: without overcoming the viscosity-induced agglomeration, agricultural waste fillers act as stress concentrators rather than reinforcement agents. Consequently, while the current F3 composite is unsuitable for structural wound dressings due to premature fracture, its high absorptive capacity suggests potential for non-load-bearing applications. Future research must prioritize high-energy dispersion techniques (e.g., ultrasonication) to resolve this microstructural defect and unlock the true reinforcement potential of rice husk cellulose.

RECOMMENDATIONS

Based on the key findings of this study—specifically the synergistic success of the F2 (PVA/Guar Gum) matrix and the catastrophic mechanical failure of the F3 cellulose composite (TS 5.48 MPa) due to agglomeration—several recommendations are proposed for future research. The primary recommendation is the mandatory replacement of the simple magnetic stirring method. Future work must utilize high-energy dispersion techniques, such as ultrasonication or high-shear homogenization, to forcibly deagglomerate the cellulose particles prior to casting. Only by achieving homogeneous particle dispersion can the true mechanical reinforcement potential of cellulose be validated. Furthermore, specific to the rice husk feedstock, the significant silica (SiO_2) bodies identified in SEM (Figure 1) must be addressed.

Although FTIR (Figure 4) indicated pure cellulose, residual silica—an inorganic impurity not detected by FTIR—likely contributes to the mechanical failure. It is recommended to quantify residual silica (e.g., via TGA or XRF) and consider an acid pre-treatment (e.g., HCl) to remove it. As an alternative to physical dispersion, cellulose surface modification (such as acetylation or grafting) could be explored to reduce inter-particle agglomeration and improve interfacial adhesion with the PVA/Guar Gum matrix [3]. Finally, regarding the F5 (Chitosan) formulation,

which showed an extreme trade-off (612.9% SR vs. 0.95 MPa TS), future work should focus on balancing these properties. While chitosan is the superior SAP candidate, its mechanical integrity must be enhanced, potentially by introducing a chemical crosslinker (e.g., glutaraldehyde) in addition to the physical freeze-thaw method, to create a viable, balanced SAP hydrogel.

ACKNOWLEDGEMENTS

The authors gratefully acknowledge the financial support from Politeknik Negeri Indramayu (Polindra), provided through a grant from the Penelitian, Pengabdian kepada Masyarakat, dan Pengembangan (P3M) unit. This funding was essential for the successful completion of this research. Sincere gratitude is also extended to all colleagues who provided technical assistance and invaluable feedback throughout this study. It is hoped that these findings will contribute to the advancement of both science and practice

BIBLIOGRAPHY

Adawiyah, R., Suryanti, V., & Pranoto. (2022). Preparation and characterization of microcrystalline cellulose from lembang (Typha angustifolia L.). *Journal of Physics: Conference Series*, *2190*(1), 12007. https://doi.org/10.1088/1742-6596/2190/1/012007

Ahearne, M. (2022). 4 - Mechanical testing of hydrogels. In H. Li & V. B. T.-T. M. of H. Silberschmidt (Eds.), *Elsevier Series in Mechanics of Advanced Materials* (pp. 73–90). Woodhead Publishing. https://doi.org/https://doi.org/10.1016/B978-0-08-102862-9.00003-8

Ahmed, E. M. (2015). Hydrogel: Preparation, characterization, and applications: A review. *Journal of Advanced Research*, *6*(2), 105–121. https://doi.org/https://doi.org/10.1016/j.jare.2013.07.006

Alonso-Cuevas, C. F., Ramírez-Guzmán, N., Serna-Cock, L., Guancha-Chalapud, M., Aguirre-Joya, J. A., Aguillón-Gutiérrez, D. R., Claudio-Rizo, A., & Torres-León, C. (2025). From Agro-Industrial Waste to Natural Hydrogels: A Sustainable Alternative to Reduce Water Use in Agriculture. In *Gels* (Vol. 11, Issue 8, p. 616). https://doi.org/10.3390/gels11080616

Azzouni, D., Alaoui, S., Bertani, R., Alanazi, M., En-Nabety, G., & Taleb, A. (2024). Experimental and Theoretical Investigation of the Inhibitor Efficiency of Eucalyptus globulus Leaf Essential Oil (EuEO) on Mild Steel Corrosion in a Molar Hydrochloric Acid Medium. *Molecules*, *29*, 3323. https://doi.org/10.3390/molecules29143323

Brand, I. (2020). *Polarization Modulation Infrared Reflection Absorption Spectroscopy: From Theory to Experiment BT - Application of Polarization Modulation Infrared Reflection Absorption Spectroscopy in Electrochemistry* (I. Brand (ed.); pp. 7–45). Springer International Publishing. https://doi.org/10.1007/978-3-030-42164-9_2

Chen, J., Shi, X., Ren, L., & Wang, Y. (2017). Graphene oxide/PVA inorganic/organic interpenetrating hydrogels with excellent mechanical properties and biocompatibility. *Carbon*, *111*, 18–27. https://doi.org/https://doi.org/10.1016/j.carbon.2016.07.038

Dai, F., Zhuang, Q., Huang, G., Deng, H., & Zhang, X. (2023). Infrared Spectrum Characteristics and Quantification of OH Groups in Coal. *ACS Omega*, *8*(19), 17064–17076. https://doi.org/10.1021/acsomega.3c01336

Elsaeed, S. M., Zaki, E. G., Abdelhafes, A., & Al-Hussaini, A. S. (2022). Response Surface

Method Based Modeling and Optimization of CMC-g Terpolymer Interpenetrating Network/Bentonite Superabsorbent Composite for Enhancing Water Retention. *ACS Omega*, *7*(10), 8219–8228. https://doi.org/10.1021/acsomega.1c03194

Farrukh, S., Fan, X., Karim, S. S., Yu, Z., & Lu, G. (2025). Synergistic effects of structured and powdered Calcium Chloride-Activated Carbon composites on Ammonia adsorption: the role of salt distribution and pH-controlled crosslinking. *Emergent Materials*, *8*(6), 5217–5240. https://doi.org/10.1007/s42247-025-01106-8

Górska, A., Baran, E., Knapik-Kowalczuk, J., Szafraniec-Szczęsny, J., Paluch, M., Kulinowski, P., & Mendyk, A. (2024). Physically Cross-Linked PVA Hydrogels as Potential Wound Dressings: How Freezing Conditions and Formulation Composition Define Cryogel Structure and Performance. *Pharmaceutics*, *16*(11). https://doi.org/10.3390/pharmaceutics16111388

Guo, L., Sato, H., Hashimoto, T., & Ozaki, Y. (2010). FTIR Study on Hydrogen-Bonding Interactions in Biodegradable Polymer Blends of Poly(3-hydroxybutyrate) and Poly(4-vinylphenol). *Macromolecules*, *43*. https://doi.org/10.1021/ma100307m

Himawan, A., Korelidou, A., Pérez-Moreno, A. M., Paris, J. L., Dominguez-Robles, J., Vora, L. K., Permana, A. D., Larrañeta, E., Graham, R., Scott, C. J., & Donnelly, R. F. (2025). Formulation and evaluation of PVA-based composite hydrogels: physicochemical, leachables, and in vitro immunogenicity studies. *Journal of Materials Chemistry B*, *13*(7), 2431–2445. https://doi.org/10.1039/d4tb02181a

Hishikawa, Y., Togawa, E., & Kondo, T. (2017). Characterization of Individual Hydrogen Bonds in Crystalline Regenerated Cellulose Using Resolved Polarized FTIR Spectra. *ACS Omega*, *2*(4), 1469–1476. https://doi.org/10.1021/acsomega.6b00364

Hoerudin, H., Setyawan, N., Suismono, Purwaningsih, H., & Apriliani, N. (2022). Morphology, Extraction Yield, and Properties of Biogenic Silica Nanoparticles from Indonesian Rice Husk as Influenced by Solvent Type and Aging Time. *IOP Conference Series: Earth and Environmental Science*, *1024*, 12076. https://doi.org/10.1088/1755-1315/1024/1/012076

Irianto, H. E., Riastuti, R., Pangesty, A. I., & Nugraha, A. F. (2024). *Extraction and Characterization of Micro-fibrillated Cellulose from Rice Husk Waste for Biomedical Purposes*. *15*(August 2023), 342–352. https://doi.org/10.14716/ijtech.v15i2.6698

Lee, D., Park, J., Hwang, K., Chun, S.-J., Kim, J. H., Lee, T.-J., Lee, B.-T., Cho, H.-J., Kim, B.-J., Wu, Q., & Gwon, J. (2024). Poly(vinyl alcohol) Hydrogels Reinforced with Cellulose Nanocrystals for Sustained Delivery of Salicylic Acid. *ACS Applied Nano Materials*, *7*(4), 3918–3930. https://doi.org/10.1021/acsanm.3c05526

Lin, X., Zhao, X., Xu, C., Wang, L., & Xia, Y. (2022). Progress in the mechanical enhancement of hydrogels: Fabrication strategies and underlying mechanisms. *Journal of Polymer Science*, *60*(17), 2525–2542. https://doi.org/https://doi.org/10.1002/pol.20220154

Liu, Y., & Chan, K. H. (n.d.). *Advances in Hydrogels*.

Mamudu, U., Kabyshev, A., Bekmyrza, K., Kuterbekov, K. A., Baratova, A., Omeiza, L. A., & Lim, R. C. (2025). Extraction, Preparation and Characterization of Nanocrystalline Cellulose from Lignocellulosic Simpor Leaf Residue. *Molecules (Basel, Switzerland)*, *30*(7). https://doi.org/10.3390/molecules30071622

Merisha, M., Jasvy, S., Lesly Fathima, A., Santhamoorthy, M., Asaithambi, P., Thirupathi, K., & Phan, T. T. V. (2025). A comprehensive review of the fabrication of chitosan nanoparticles and their applications in environmental and biomedical sciences. *Journal of*

Macromolecular Science, Part A, *62*(11), 953–972. https://doi.org/10.1080/10601325.2025.2568711

Mieles-Gómez, L., Quintana, S. E., & García-Zapateiro, L. A. (2021). Development of new eggplant spread product: A rheological and chemical characterization. *Heliyon*, *7*(8), e07795. https://doi.org/https://doi.org/10.1016/j.heliyon.2021.e07795

Mohanty, S. S., Pati, S., & Samal, S. K. (2025). *Recent Advancement of Sustainable Scaffolds in Regenerative Medicine BT - Sustainable Scaffolds-based Strategies in Tissue Engineering and Regenerative Medicine* (J. M. Oliveira, J. Silva-Correia, & R. L. Reis (eds.); pp. 3–45). Springer Nature Switzerland. https://doi.org/10.1007/978-3-031-96274-5_1

Paramitha, V. W., & Maharani, D. K. (2025). *Isolation and Characterization of Nanocellulose from Rice Husk (Oryza sativa L .) Waste Through Chemical and Ultrasonication Treatment*. *20*(6), 1043–1047.

Park, J. Y., Gu, Y. M., Chun, J., Sang, B. I., & Lee, J. H. (2023). Pilot - scale continuous biogenic silica extraction from rice husk by one - pot alkali hydrothermal treatment and ball milling. *Chemical and Biological Technologies in Agriculture*, 1–7. https://doi.org/10.1186/s40538-023-00479-4

Shivasharanappa, K., Hanchinalmath, J. V, Shivakumar, S., Kudva, S., Jain, S. C., Girish, M., Wijekoon, D. G. W. M. H. M. M., Dutta, R., Pramod, T., & Patil, S. J. (2022). *Rice Husk as a Source of Nutraceuticals BT - Food and Agricultural Byproducts as Important Source of Valuable Nutraceuticals* (C. Egbuna, B. Sawicka, & J. Khan (eds.); pp. 215–225). Springer International Publishing. https://doi.org/10.1007/978-3-030-98760-2_15

Sinamo, S., Tarigan, S., Gea, S., & Putra, D. P. (n.d.). *Bioscientia Medicina : Journal of Biomedicine & Translational Research Utilization of Silica Nanoparticles from Rice Husks for Improving the Mechanical Properties of Dental Materials : A Literature Review*. 2644–2650.

Somseemee, O., Saeoui, P., Schevenels, F. T., & Siriwong, C. (2022). Enhanced interfacial interaction between modified cellulose nanocrystals and epoxidized natural rubber via ultraviolet irradiation. *Scientific Reports*, *12*(1), 6682. https://doi.org/10.1038/s41598-022-10558-5

Sørensen, B. F. (2024). 11 - Delamination fracture in composite materials. In R. Talreja & J. B. T.-M. D. Varna Fatigue and Failure of Composite Materials (Second Edition) (Eds.), *Woodhead Publishing Series in Composites Science and Engineering* (pp. 221–251). Woodhead Publishing. https://doi.org/https://doi.org/10.1016/B978-0-443-18489-5.00001-1

Stan, D., Mirica, A.-C., Mocanu, S., Stan, D., Podolean, I., Candu, N., El Fergani, M., Stefan, L. M., Seciu-Grama, A.-M., Aricov, L., Brincoveanu, O., Moldovan, C., Bocancia-Mateescu, L.-A., & Coman, S. M. (2025). Hybrid Hydrogel Supplemented with Algal Polysaccharide for Potential Use in Biomedical Applications. *Gels*, *11*(1). https://doi.org/10.3390/gels11010017

Sultana, N., Hasan, M., Habib, A., Saifullah, A., Azim, A. Y. M. A., Alimuzzaman, S., & Sarker, F. (2023). Short Jute Fiber Preform Reinforced Polypropylene Thermoplastic Composite: Experimental Investigation and Its Theoretical Stiffness Prediction. *ACS Omega*, *8*(27), 24311–24322. https://doi.org/10.1021/acsomega.3c01533

Tamahkar, E., & Ozkahraman, B. (2015). *Potential Evaluation of PVA-Based Hydrogels for Biomedical Applications*. *2*(2), 165–171. https://doi.org/10.17350/HJSE19030000021

Uchida, M., Sato, H., Kaneko, Y., Okumura, D., & Hossain, M. (2025). Evaluation of intermolecular interactions of hydrogels: Experimental study and constitutive modeling. *International Journal of Solids and Structures*, *317*, 113428. https://doi.org/https://doi.org/10.1016/j.ijsolstr.2025.113428

Wang, G., Jiang, G., Zhu, Y., Cheng, W., Cao, K., Zhou, J., Lei, H., Xu, G., & Zhao, D. (2022). Developing cellulosic functional materials from multi-scale strategy and applications in flexible bioelectronic devices. *Carbohydrate Polymers*, *283*, 119160. https://doi.org/https://doi.org/10.1016/j.carbpol.2022.119160

Wang, M., Shao, L., & Jia, M. (2022). Shape memory and underwater superelastic mof@cellulose aerogels for rapid and large-capacity adsorption of metal ions. *Cellulose*, *29*(15), 8243–8254. https://doi.org/10.1007/s10570-022-04774-5

Wang, Q., Kudo, S., Asano, S., & Hayashi, J.-I. (2022). Fabrication of Densified Rice Husk by Sequential Hot-Compressed Water Treatment, Blending with Poly(vinyl alcohol), and Hot Pressing. *ACS Omega*, *7*(31), 27638–27648. https://doi.org/10.1021/acsomega.2c03286

Wang, R., Cheng, C., Wang, H., & Wang, D. (2024). Swollen hydrogel nanotechnology: Advanced applications of the rudimentary swelling properties of hydrogels. *ChemPhysMater*, *3*(4), 357–375. https://doi.org/https://doi.org/10.1016/j.chphma.2024.07.006

Wang, S., Lei, L., Tian, Y., Ning, H., Hu, N., Wu, P., Jiang, H., Zhang, L., Luo, X., Liu, F., Zou, R., Wen, J., Wu, X., Xiang, C., & Liu, J. (2024). Strong, tough and anisotropic bioinspired hydrogels. *Materials Horizons*, *11*(9), 2131–2142. https://doi.org/10.1039/D3MH02032K

Zhao, T., Li, X., Gong, Y., Guo, Y., Quan, F., & Shi, Q. (2021). Study on polysaccharide polyelectrolyte complex and fabrication of alginate/chitosan derivative composite fibers. *International Journal of Biological Macromolecules*, *184*, 181–187. https://doi.org/https://doi.org/10.1016/j.ijbiomac.2021.05.150

Zhao, Z., Li, Y., Li, Y., & Song, X. (2025). Hydrogels May Not Always Absorb Water: Strategies to Achieve Antiswelling and Negative Swelling. *ChemPhysChem*, *n/a*(n/a), e202500446. https://doi.org/https://doi.org/10.1002/cphc.202500446